156 CONFIRMING BOTTOM-UP TORNADOGENESIS IN THE 31 MAY 2013 EL RENO, OK TORNADO

Jana Houser[1,1], Anton Seimon[2], Kyle Thiem[3,4], Howard Bluestein[4], Jeff Snyder[5], Skip Talbot and John Allen[6]

[1] Ohio University, Athens, OH
[2] Appalachian State Univeristy, Boone, NC
[3] National Weather Service, Peachtree City, GA
[4] University of Oklahoma, Norman, OK
[5] National Severe Storms Laboratory
[6] Central Michigan University

1. INTRODUCTION:

For more than forty years, one of the primary processes believed to be responsible for forming tornadoes in supercell thunderstorms was the 'top down', or 'descending' process, which explains the gradual descent of strong rotation from mid-levels of the storm to the surface via the dynamic pipe effect. This theory originated from early simulations by Leslie (1971) and Smith and Leslie (1978), that were supported by observations from the 'new' Doppler radar in central Oklahoma (Burgess 1975; Brown et al. 1978). The theory suggests that strong rotation develops several km above the ground, which dynamically generates a perturbation low pressure, inducing an updraft immediately below this strong rotation. Convergence into the updraft enhances rotation below the original area of rotation through the conservation of angular momentum. Once rotational flow has accelerated and cyclostrophic balance is achieved, the rotation continues to build downward, essentially being drawn up from below into the region of strong rotation until a column of rotating air intersects the ground, at which time a tornado forms. A later study of 52 tornadoes observed by WSR-88D radars performed by Trapp et al. (1999) indicated that 52% of all tornadoes analyzed formed with descending tornado vortex signatures (TVSs), a proxy for the identification of the top-down method. Of those tornadoes 52 tornadoes, 40 formed from supercell storms, and from that sub-population, 67 percent were deemed to have formed via the top-down process. Conclusions from this study suggest that the primary mode for tornadogenesis from supercells still is descending.

However, with the advent of new rapid-scan technology (e.g. Pazmany et al. 2013), these results have been called into question. French et al. (2013) and Houser et al. (2014, 2015) concluded that the tornadoes they observed (6 collectively) did NOT form from the descending process. Rather, they formed either from the bottom up, or via the simultaneous contraction of a deep layer of rotation that quickly – over a mere 30 – 90 s – strengthened to tornadic intensity. A subsequent study by French et al. (2014) further found strong evidence that when the descending process is observed by WSR-88D radars, it is the result of poor temporal resolution degrading the spatio-temporal evolution of the rotation, spuriously attributing short-lived, transient vortices to the parent tornado vortex.

While the French et al. and Houser et al. studies have triggered a shift in the tornadogenesis paradigm away from the descending method, there has been a paucity of near-ground-level observations acquired from rapid-scanning instruments to fill in the gaps of what is happening with the evolution of rotation at the surface.

On 31 May 2013, a large, fatal tornado occurred near El Reno Oklahoma. This tornado

[1] *Corresponding author address:* Dr. Jana Houser, Department of Geography, Ohio University, Athens, OH. Email: houserj@ohio.edu

was unusual for several reasons including the fact that it reached a record 4.2 km (2.6 miles) wide, initially had a southeasterly track, had radar-observed wind speeds > 135 m/s (>300 mph), (Bluestein et al. 2015) and catastrophically resulted in the fatality of three veteran storm chasers (Wurman et al. 2014). This tornado was observed at unusually low-levels by the Rapid-Scan, X-band, Polarimetric mobile radar (RaXPol) (Pazmany et al. 2013), and a plethora of visual documentation of the tornado acquired from diverse viewing angles of the storm was collated with unprecedented accuracy and coverage in the El Reno Survey (Seimon et al. 2016). The combination of low-level rapid-scan radar observations coupled with the visual observations from the El Reno Survey enabled a unique examination and comparison of the evolution of rotation associated with the tornado as it was forming.

2. INSTRUMENTATION AND METHODOLOGY

Radar data were acquired from the RaXPol mobile radar platform. RaXPol is capable of scanning a 360° PPI in 2 s and the data are time stamped based upon an internal GPS-based clock with accuracy ~ 1 s. During this deployment, 12 360° PPI's were collected at elevation angles ranging from 0° to 20°, at 2° increments with an additional PPI added to allow the antenna to transition back to 0°. Thus, volumetric updates were available every ~29 s. The radar was deployed about 10 km away from the tornadogenesis location (Fig. 1). The deployment location of the radar, which was slightly elevated with a relatively unimpeded

Fig. 1: Deployment location of the RaXPol prior to tornadogenesis on 31 May, 2013. The parent supercell is seen in the backgrounds. Photo © Tracie Seimon

view to the west, towards the developing tornado, enabled data collection at the 0° elevation angle. These data, while only mildly impacted by ground clutter from beam spreading, were sampled at heights < 50 m above ground level (AGL), and as low as ~20 m AGL, promoting extremely fine spatio-temporal resolution observations of the tornadogenesis process very near the ground. For additional details about deployment location and the dataset, the reader is referred to Bluestein et al. (2015.)

In order to analyze the evolution of rotation associated with the tornado as it was forming and immediately prior to genesis, the tornado vortex signature (TVS) was identified in each radar scan. For the purposes of this study, a TVS was defined as a difference in maximum inbound and outbound Doppler velocities (ΔV_{max}) that exceeded 40 m s^{-1} over an azimuthal distance less than 1 km. Analysis began when there was an obvious TVS present at all elevation angles. The TVS was then tracked backward with time until it was no longer visible in the data. Additionally, the strength of the mesocyclone rotation was included in a different dataset when a TVS was not present. This inclusion promoted insight into the evolution of the larger, storm-scale rotation enabling analysis of how the strength of the low-level mesocyclone also changed in time prior to tornadogenesis. Mesocyclone strength was similarly evaluated using ΔV_{max}, except there was no specific threshold for intensity that had to be met. There merely had to be an observed maximum in inbound and outbound velocities within 6 km of each other.

Visual observations of the storm were acquired from the Tornado Environment Display web-based tool, generated by the El Reno Survey (http://el-reno-survey.net/ted/). This project used crowd-sourced videos from storm chasers who were documenting the El Reno tornado, precisely geolocating the individuals using GPS logs and georeferencing techniques (within 5 m). Furthermore, videos were formatted to be contemporaneous with each other to within .033 s using lightning flashes as temporal reference points. The TED tool enables users to select videos based upon GPS icons, displaying up to 4 videos simultaneously. These videos are layered over the WSR-88D radar imagery with overlays of

storm chaser locations (Fig. 2). For additional details, the reader is referred to Seimon et al. (2016).

Fig. 2: Example of the web-based TED tool. Temporally and geo-synchronized video from up to 4 storm chasers can be displayed at the same time. The background image is the KTLX WSR-88D radar imagery valid at the time the videos are rolling, and storm chaser locations (blue triangles) are superimposed upon the radar image, with a Google Earth map of the area as the base layer. The user can choose which video to show in the screen by selecting the GPS icon on the background image, or selecting the user from a drop-down menu.

3. RESULTS:

Based upon the visual database collected by the El Reno Survey, a condensation funnel was observed to be in contact with the ground at 2302:25 (Fig. 3). However, based upon the preliminary work by Bluestein et al. (2015), the radar-based time of tornadogenesis was around 2304. The radar-derived time was based off of the observations of a vertically continuous TVS over the depth of the radar-observed domain (~ 3.5 km).

Fig. 3: Screen capture of video taken by Heidi Farrar on 31 May 2013 clearly documenting a condensation funnel with debris at 2302:25. © H. Ferrar.

Upon closer investigation, it was determined that the ONLY evidence of a TVS that was present in the radar data at the time the condensation funnel was first seen, occurred in the 0° elevation angle data. This corresponded with a height of ~30 m above ground level (AGL). Furthermore, there were considerable differences between the near-tornado flow field at 0° and at 2°, which was the next lowest data point available, corresponding with a height of ~ 300 AGL (Fig. 4). It is seen from the radar imagery at 2300:50 that rotation at 0° began to contract prior to the contraction of the broad cyclonic shear associated with the low-level mesocyclone at 2°. The rotation at 0° met the definition of a TVS at 2302:17 (not shown), and it proceeded to intensify with time. By 2303:43, a TVS was also present in the 2° data.

When evaluating the evolution of the TVS with time and height, it is clear that the rotation developed first near the surface, at the 0° elevation, and then proceeded rapidly upward with height over a short period of time (~60 s) (Fig. 5). There was no evidence of a TVS aloft from any other elevation angle in the vicinity of the nascent tornado prior to the development of the vertically coherent vortex. This result provides strong evidence against the descending vortex mechanism, and for a bottom-up process in this case.

Prior to achieving tornadic strength rotation (ΔV_{max} > 40 m s^{-1}) at 0°, there was a subtornadic velocity couplet present for an additional ~90 s earlier. The visual observation of the condensation funnel temporally matched the radar scan first associated with a TVS exceeding the 40 m s^{-1} threshold at 0°. Thus, the 40 m s^{-1} threshold agrees with the visual confirmation of a tornado for this case, providing observational support for this metric, which is often used to demark tornadic vs. nontornadic velocity couplets (e.g. Marquis et al 2012; Kosiba et al. 2013).

The evolution of mesocyclone-scale rotation at times when a TVS was not present in addition to the tornado intensity when a TVS was present is given in Fig. 6. About 6 minutes prior to tornadogenesis, there was a strengthening of

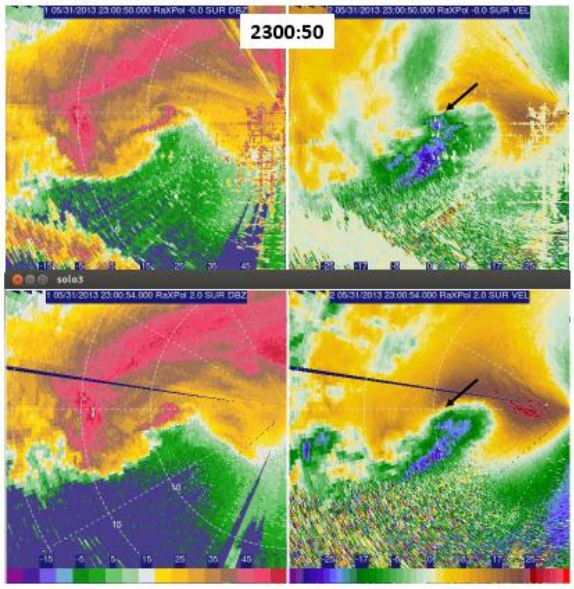

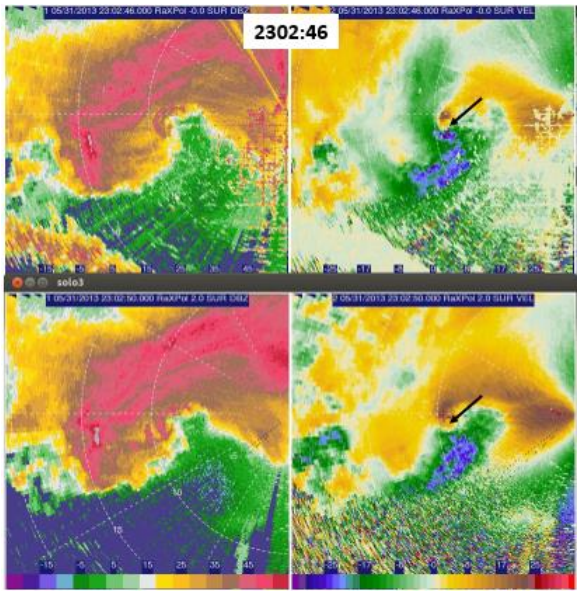

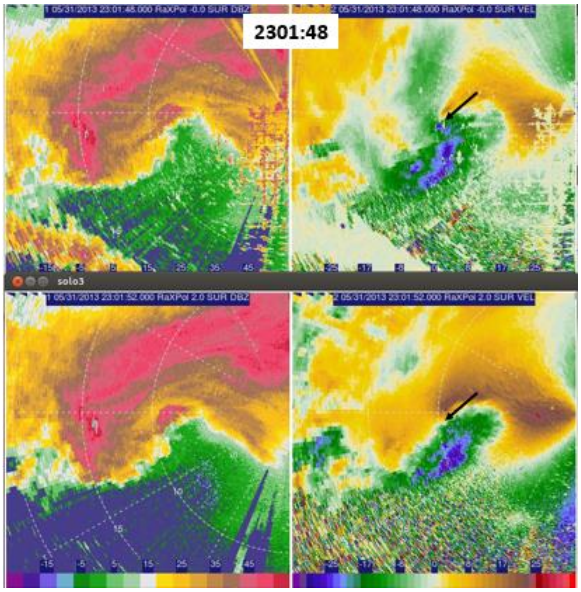

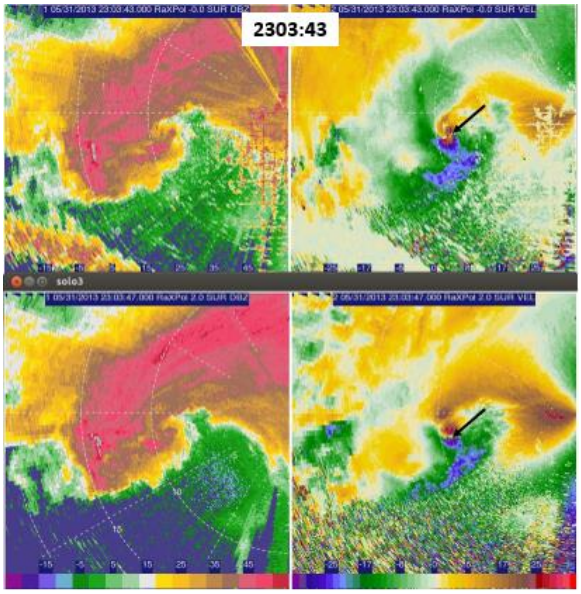

Fig. 4: (Above) Series of radar imagery from RaXPol around tornadogenesis time. The top row of images in each 4-panel series is from the 0° elevation angle while the bottom row is from 2°. The left-hand panels are reflectivity and the right-hand panels are Doppler velocities. The black arrow points to the same location at both the 0° and 2° elevation angle plots, and indicates the area where the TVS forms at 0°, then eventually at 2°.

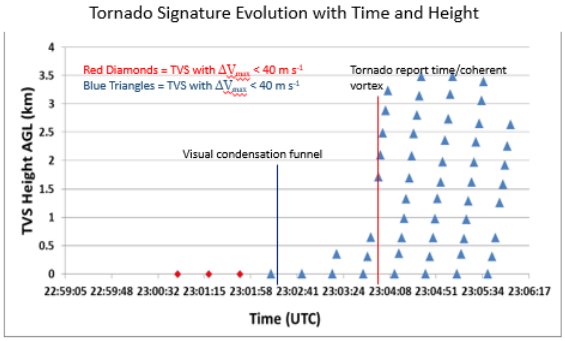

Fig. 5: (Lower right) Evolution of the TVS with time and height. Only the evolution of the TVS was tracked for this image. Blue triangles indicate a true TVS with $\Delta V_{max} > 40$ m s^{-1} while red diamonds indicate a couplet with $\Delta V_{max} > 40$ m s^{-1}.

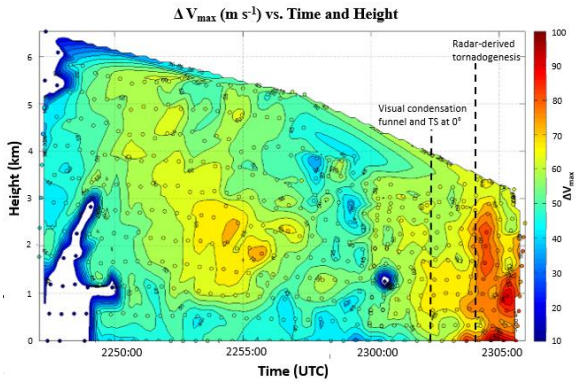

Fig. 6: Mesocyclone strength (as derived from ΔV_{max} when a TVS was not present) with time (x-axis) and height (y-axis). Colored contours indicate the strength of the rotation interpolated from specific data points (small circles).

the low-level mesocyclone between 1 and 3 km. However, this period of brief intensification did not persist through the tornadogenesis. This observation is similar to the findings of Houser et al. (2015), when they found a rather sudden, but short-lived intensification of rotation near the same heights. Interestingly, the duration between the presence of this stronger mesocyclonic rotation and the onset of tornadogenesis is approximately the same increment as the scan time between consecutive WSR-88D volumes. Thus, the descending process could potentially be inferred by a WSR-88D instrument based upon these observations.

About one to two minutes prior to the time the visual condensation funnel was on the ground, there was also an increase in the low-level mesocyclone strength, with a peak intensification between 0.75 and 2 km AGL occurring simultaneously with the visual documentation of the funnel cloud (Fig. 6). The sudden intensification of the deep-layer rotation seen around 2304 is associated with the development of the vertically continuous tornado. It is hypothesized that the intensification of the low-level mesocyclone likely played a critical role in forcing the upward directed pressure gradient force needed to generate the strong vertical motion required for tornadogenesis, as has been suggested by traditional tornadogenesis studies (e.g. Klemp and Rotunno 1983). With the strengthening of low-level rotation, low perturbation pressure is induced dynamically, which will cause a vertically-oriented upward directed pressure gradient for to occur. Such a force would accelerate air upward, into the area of low pressure above. With pre-existing rotation at or very near the surface, this upward motion would act to stretch the rotation and advect it upward, potentially rapidly forming a tornado.

4. CONCLUSIONS AND DISCUSSION:

A unique dataset from the notorious 31 May 2013 El Reno tornado combining low-level, rapid-scan radar data and a robust visual database from the El Reno Survey was used to analyze the evolution of rotation with time and height prior to and during tornadogenesis, and put the radar observations in the context of visual observations. From the results, it can be concluded that:

I. Tornadogenesis began very near the surface.

II. A condensation funnel was observed visually when the only radar-based evidence of a tornado existed in the lowest (0°) elevation angle, corresponding to a height of < 50 m AGL. A TVS was NOT observed at the next lowest elevation angle (~300 m AGL) until ~90 s after the low-level TVS.

III. The development into a vertically continuous and deep vortex occurred very rapidly (over ~60 s) and showed evidence of rapid growth from the ground up. This conclusion is in agreement with previous findings by French et al. (2013) and Houser et al. (2015).

IV. The low-level mesocyclone strengthened relatively suddenly and rapidly, prior to the development of the tornado, as is expected from traditional tornadogenesis theory (e.g. Klemp and Rotunno 1983)

V. The visual observations from the El Reno Survey played a critical role in the interpretation of the radar data.

Putting this study into context with others that have previously been done, the theory of bottom-up or nondescending tornadogenesis is not new. However, observational support for tornadogenesis processes has been relatively

hard to come by, predominately owing to the challenge of collecting high quality data at the right time and location to capture tornadogenesis. Furthermore, the capability of radars to collect data on the short time scales over which tornadoes evolve is a relatively new accomplishment. Thus, this study contributes to the state of the science by providing a high quality, visually-supported observational dataset that definitively answers the question of how rotation evolved with time and height for this tornado.

It is important to note that this is a single sample and is likely not representative of the whole tornado population. However, it provides evidence from yet another storm that the descending mechanism is not observed, and it has yet to be observed in rapid-scan datasets.

5. REFERENCES:

Bluestein, H., J. Snyder, and J. Houser, 2015: A multiscale overview of the El Reno, Oklahoma tornadic supercell of 31 May 2013. *Mon. Wea. Rev.,* **30,** 525-552.

Brown, R. A., L. R. Lemon, and D. W. Burgess, 1978: Tornado detection by pulsed Doppler radar. *Mon. Wea. Rev.*, **106**, 29–38.

Burgess, D. W., L. R. Lemon, and R. A. Brown, 1975: Tornado characteristics revealed by Doppler radar. *Geophy. Res. Lett.,* **2**, 183-184.

French, M. M., H. B. Bluestein, I. Popstefanija, C. A. Baldi, and R. T. Bluth, 2013: Reexamining the vertical development of tornadic vortex signatures in supercells. *Mon. Wea. Rev.,* **141**, 4576–4601.

——, ——, ——, ——, and ——, 2014: Mobile, phased-array, Doppler radar observations of tornadoes at X-band. *Mon. Wea. Rev.,* **142**, 1010–1036

Houser, J. B., H. B. Bluestein, and J. C. Snyder, 2014: A comparison of the evolution of strong low-level rotation associated with tornadogenesis and tornadogenesis failure observed by rapid-scan Doppler radar. *27th Conf. on Severe Local Storms*, Amer. Meteor. Soc., Madison, WI.

_____, _____, and _____ 2015: Rapid-scan, polarimetric, Doppler radar observations of tornadogenesis and tornado dissipation in a tornadic supercell: The ‘‘El Reno, Oklahoma’’ storm of 24 May 2011. Mon. Wea. Rev., 143, 2685– 2710

Klemp, J, and R. Rotunno, 1983: A study of the tornadic region within a supercell thunderstorm. *J. Atmos. Sci.*, **40**, 359–377.

Kosiba, K. A., J. Wurman, Y. Richardson, P. Markowski, and P. Robinson, 2013: Genesis of the Goshen County, Wyoming, tornado on 5 June 2009 during VORTEX2. *Mon. Wea. Rev*.,**141**, 1157–1181.

Leslie, L. M., 1971: “The development of concentrated vortices: a numerical study. *J. Fluid. Mech.* **48,** 1-21.

Marquis, J., Y. Richardson, P. Markowski, D. Dowell, and J. Wurman, 2012: Tornado maintenance investigated with high-resolution dual-Doppler and EnKF analysis. *Mon. Wea. Rev.,* **140**, 3–27.

Pazmany, A. L., J. B. Mead, H. B. Bluestein, J. C. Snyder, and J. B. Houser, 2013: A mobile rapid-scanning X-band polarimetric (RaXPol) Doppler radar system. J. Atmos. Oceanic Technol., 30, 1398–1413

Seimon, A., J. Allen, T. Seimon, S. Talbot, and D. Hoadley, 2016: Crowdsourcing the El Reno 2013 tornado: A new approach for collation and display of storm chaser imagery for scientific applications. *Bull. Amer. Meteor. Soc.*, **97,** 2068-2084.

Smith, R. K. and L. M. Leslie, 1978. Tornadogenesis. *Quart. J. Roy. Meteor. Soc.,* **105,** 107-127.

Trapp, R. J., E. D. Mitchell, G. A. Tipton, D. W. Effertz, A. I. Watson, D. L. Andra, and M. A. Magsig, 1999: Descending and nondescending tornadic vortex signatures detected by WSR-88Ds. *Wea. Forecasting*, **14**, 625–639.

Wurman, J., K. Kosiba, P. Robinson, and T. Marshall, 2014: The role of multiple-vortex tornado structure in causing storm researcher fatalities. *Bull. Amer. Meteor. Soc., **95**, 31-45.*